This is a chapter contributed to the book: Bioelectromagnetics in Healthcare Advanced sensing and communication applications. Published by Scitech (an imprint of the IET) 2022. ISBN: 978-83953-349-5.

Chapter 10

Epidermal and Conformal Electronics for Bio Sensing Applications

John Batchelor[1], Viktorija Makarovaite[1] and Robert Horne[1]

This chapter is concerned with low power epidermally or conformally mounted flexible sensing tags that use passive backscattered communications links with the UHF Gen2 RFID protocol (865–928 MHz) [1]. Very low-profile polymer or fabric substrate skin mountable UHF RFID tag designs were introduced by [2], with proposed fabrication by inkjet printing [3], and incorporation of sensing [4], while alternatively, integrated, flexible silicon NFC sensing systems at 13.56 MHz have been pioneered by [5].

The high permittivity and loss of human tissue [6] together with the requirement for epidermal tags to stretch and allow the skin to breath, mean that RFID tags must factor in mechanical as well as electromagnetic considerations, [7]. Appropriate substrate materials must be used, with conductors able to flex and stretch, while reliable component mounting needs to be achieved in a system that protects the skin from soreness and exposure to irritants or toxic materials. There are several challenges, including reliability, energy consumption and scalability to overcome before implementing UHF RFID technology within the healthcare sector. Beyond UHF, RFID-5G combination using antenna arrays has been considered in [8] to compare read range and data rates at 3.6, 28 and 60 GHz and proposing that above 6 GHz, arrays offer longer read range and beamsteering advantages, while 3.6 GHz designs compare well with UHF performance for single element antennas. Some such arrays have been described in [9,10], which showed that onbody application of tags at 5G bands could achieve a 6 m read range in passive mode with performance comparable between a UHF antenna, a single dipole at 5.8 GHz and a 23-element array at 60 GHz. Finally, utilising rigid circuit board based battery-assisted UHF RFID (866 MHz) tags as wearable 9-axis accelerometry sensors has also been demonstrated for pelvis and torso mounting [11].

Section 10.1 will consider the design and initial testing of a UHF tag to sense the onset of biofilm growth resulting from a fungal infection on a throat valve prosthesis, and Section 10.2 will describe how low power streaming data can be

obtained over backscattered links using the Gen2 protocol. Section 10.3 concludes the chapter.

10.1Throat prosthesis biofilm sensing tag design

Here we describe an antenna directly mounted onto an implant as part of a proposed fungal infection management system, Figure 10.1. The antenna is part of a sensing tag located within the oesophagus at neck level. The passive tag is activated by an external reader antenna mounted a short distance from the throat. The UHF RFID implant antenna was originally designed for direct epidermal mounting on the arm based on [12]. Figure 10.2 shows the original 30 mm diameter skin mounted antenna design (dimensions provided in Table 10.1), which was a curved and convoluted dipole centred on a proximity coupled shunt capacitance matching network. The tag used a Higgs-3 RFID transponder chip with an input impedance $Z_c = 31 - j216$.

Adjusting the arm-mounted original antenna substrate thickness between 1.1 and 1.5 mm in Figure 10.2 (B) reduces aperture field coupling with the skin and improves efficiency for individuals with high muscle content (permittivity above 30). This helps reduce the need for tailored sensor antenna geometry adjustments to suit electrical parameter variations between different users. The antenna was tested on the skin of three volunteers with different body types and with the measured tissue electrical characteristics indicated in Table 10.2. The objective was

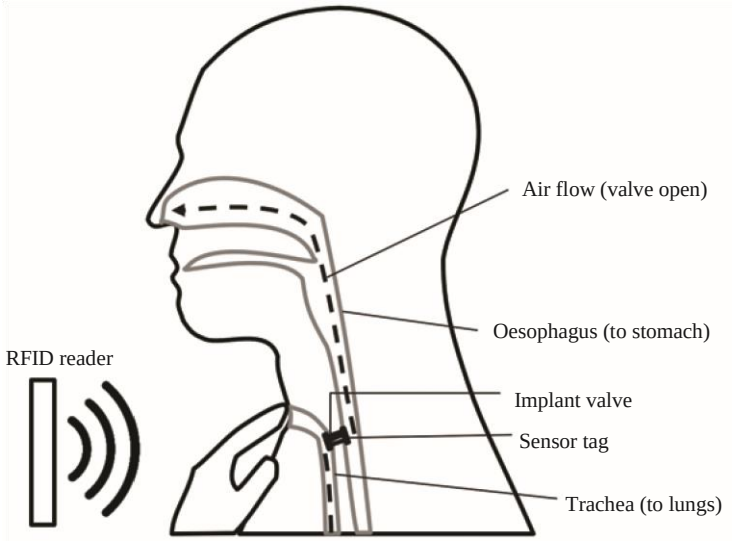

Figure 10.1 Voice prosthesis placement after a tracheostomy allowing speech to occur with blockage of the stoma (shown by utilising a finger to block stoma)

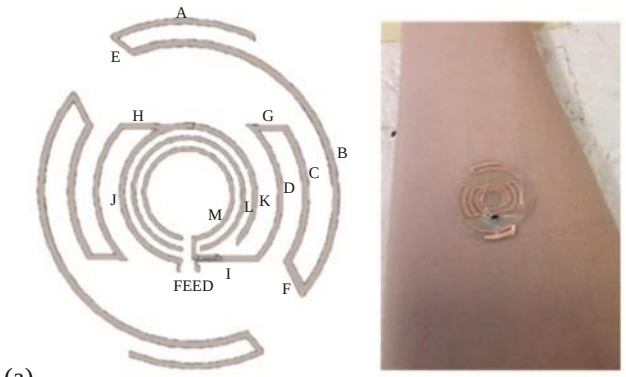

(a)

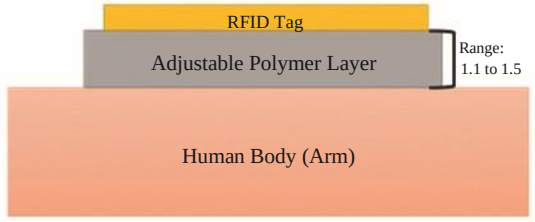

(b)

Figure 10.2 *Epidermal skin UHF RFID tag design. (A) Copper etched mylar tag (0.2 mm thickness) on body with an adjustable thickness polymer backing. (B) Representation of 1.1–1.5 mm adjustable polymer substrate between UHF RFID tag and body*

Table 10.1 *Antenna dimensions for Figure 10.2 in mm*

A	B	C	D	E	F	G	H	I	J	K	L	M
15	33	12	12.5	3.3	3.7	3.5	5	6	13	13.5	23	20

Table 10.2 *SPEAG probe dielectric measurement of volunteer forearms related to BMI and substrate thickness required to achieve 50 cm read range. Taken at 865 MHz*

Volunteer	BMI	Relative permittivity (294.25 K)	Conductivity (S/m)	Polyurethane substrate thickness (mm)
1 (thin female)	20.6	22	0.27	1.1
2 (overweight male)	27.2	30	0.42	1.1
3 (muscular male)	24.6	41	0.67	1.5

*All readings represents averaged values taken in triplicate.

***Source*: data from [14].

to determine the thickness of the antenna polyurethane layer required to achieve at least 50 cm passive backscatter read range on each individual volunteer.

A Voyantic TagformancePro calibrated system was used to indicate that an antenna substrate of just 1.1 mm is required for individuals with lower permittivity skin tissue, though an increase to 1.5 mm is needed where the permittivity rises to higher values (Figure 10.3). It is known that the high permittivity value of muscle causes greater detuning and attenuation in skin mounted antenna performance for muscular individuals than for both low and higher fat body types where there is less musculature [13] and this means that tag selection to match different individuals cannot be based on BMI alone, but should also be informed by body type.

The antennas must be tuned to account for the strong loading effect of the skin and the matched range is severely reduced when they are not attached (in air), Figure 10.3. The 'air' measurement was taken to determine consistency between the replicate tags and to account for any etching variability (leading to differing impedance mismatch and ohmic losses); no noticeable variability was seen between replicate tags when they are not attached to users. Therefore, the differences observed in read range in Figure 10.3 are accounted for by variation in user tissue composition, and any epidermal tag design characterised on a single volunteer is not an adequate indication of universal functionality. Multiple volunteers or a range of simulated dielectric phantoms must be used to demonstrate wider antenna performance.

The simulated radiation efficiencies of the arm-mounted antenna (Figure 10.2) on the 1.1 mm thick substrate were found to be 7 dB and 14 dB for volunteer 1 (thin female, ε_r = 22, S = 0.27 Sm^{-1}) and 3 (muscular male, ε_r = 41, S = 0.67 Sm^{-1}), respectively. These values are in the range expected for low profile skin mounted antennas where efficiencies can fall as low as 20 dB. An efficiency lower than 20 dB is regarded as acceptable as the human body is a

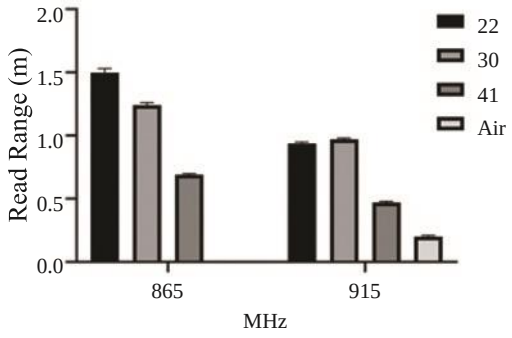

Figure 10.3 Epidermal tag measured on volunteer forearms showing that 50 cm minimum read range can be achieved for the three volunteers, thin to muscular body types (Table 10.2), with a slight adjustment in tag backing thickness as to decouple the tag from skin. Measured data represents triplicate repeats (source data from [14])

highly lossy material. However, if the tag efficiency is below 30 dB, the design will need improvement as it is unlikely to be medically useful at the chosen frequency. This is largely due to impedance mismatch and maximum read range falling below 20 cm for passive on-body UHF tags. A simple fix for impedance mismatch, to a certain degree, could be to scale the tag dimensions. This however will often have minimum effect on ohmic losses and adjustment to the tag geometry, material, adding lumped matching network components (i.e. shunting [15]) or increasing the tag separation from the lossy human tissue will be necessary [16].

Having established the antenna design to function on skin, it was reduced in diameter to 22 mm and retuned for direct mount on a PDMS elastomer throat prosthesis as indicated in Figure 10.4 with the dimensions in Table 10.3 [17]. It was initially necessary to include a 2.2 pF capacitor across the feed gap in order to tune the reduced size antenna for simulation purposes; however, during measurements,

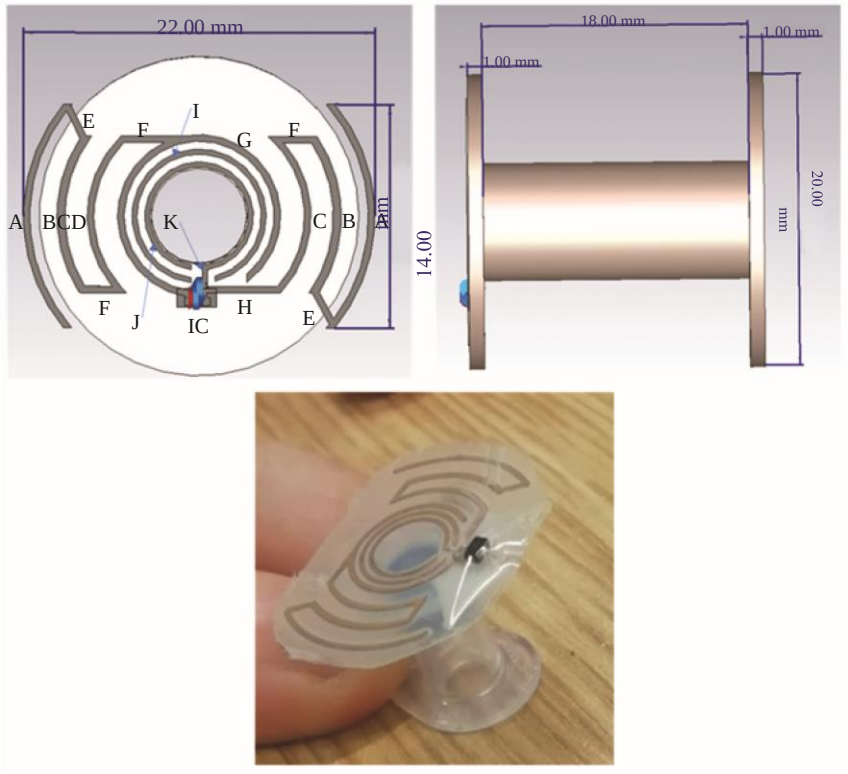

Figure 10.4 UHF RFID voice prosthesis tag design for real-time detection of microbial detection while within a body (phantom). The tag prototype consisted of a 22 mm by 14 mm meandered circular dipole etched in copper on a standard polymer voice prosthesis

Table 10.3 Antenna dimensions for Figure 10.4 in mm

A	B	C	D	E	F	G	H	I	J	K
15	8	8	12	2.8	2.5	16	4.5	23	18	2.3

it was found that capacitive loading of the gelatin phantom reduced the resonant frequency eliminating the need for the tuning component.

The purpose of the prosthesis tag is to indicate the presence of a biofilm associated with an establishing infection of the micro-organism *Candida albicans*. This fungal infection is commonly associated with the premature failure of voice prosthesis implants and can require surgical intervention for replacement [18]. Therefore, early detection of a newly establishing fungal colony improves the chances of medically treating the infection before a mature biofilm forms that would compromise the mechanical function of the implant, usually by impeding the movement of a phalange which switches air movement between the two states of speech or breathing. The passive sensing system proposed here would enable the prosthesis user to self-check the infection status and seek medical intervention as needed. The detection mechanism exploits the hydrophobic nature of the *C. albicans* biofilm, which displaces the saliva layer that would typically cover an uninfected prosthesis. Exploiting the displacement of the high permittivity saliva facilitates the detection of immature biofilms of around 5–10 mm thickness which occur in the first 4 h of a new infection. The sensor placement on the prosthesis between a substrate and superstrate, the biofilm, and a saliva layer are shown in Figure 10.5.

The antenna was covered with a 10 mm thick polymer superstrate to isolate the conductive material from the user tissue. Therefore, before the formation of a biofilm, the saliva layer lies 10 mm from the antenna and couples strongly with its aperture fields. The loading effect on the polymer mounted antenna is significant as saliva has respective relative permittivity and conductivity of around 40 and 0.3 Sm^1 at UHF frequencies, respectively. However, the aperture field-saliva coupling diminishes as an emerging biofilm pushes the saliva further from the antenna layer. The sensor functions through tracking the frequency detune that occurs as the saliva is displaced. This is manifest as a change in the tag transponder energy required from the reader, which correlates to biofilm thickness.

The sensing process is demonstrated using a physical salt and gelatin neck phantom with an embedded throat implant. For testing purposes, the hydrophobic biofilm is represented by applying 10–100 mm layers of polyurethane tape over the surface of the tag antenna. An upper limit of 100 mm was chosen as it approaches the maximum thickness of a *C. albicans* biofilm before shedding starts to occur, while 0–50 mm thickness presents normal growth over 48 h [6]. A 10 mm saliva layer was added by a pipette to form the top layer. Figure 10.6 shows the neck phantom at a fixed 30 cm from the external reader antenna. The implant has been inserted into the centre of the phantom at a point where a vertical air column

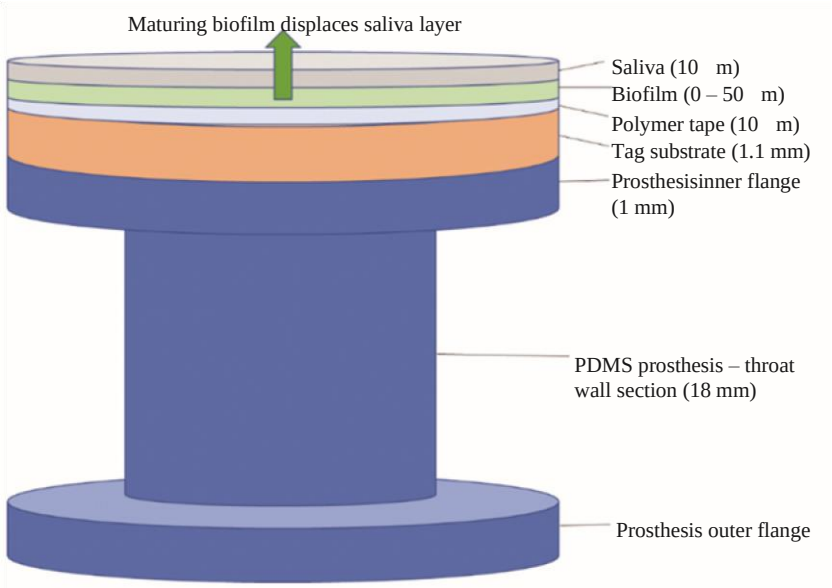

Figure 10.5 UHF RFID voice prosthesis sensing structure and biofilm. The design consisted of a 10 mm *polymer superstrate over the tag substrate which was placed on the upper portion of the voice prosthesis body (facing away from the stoma opening). An adjustable 'biofilm layer' demonstrates the tag can detect fungal biofilm growth by decoupling the uppermost saliva layer from the antenna over time*

representing the trachea intersects with a horizontal air tube representing the surgical stoma in the throat. As stated, the biofilm was represented by layers of polyurethane tape which reasonably models the characteristics of the polysaccharide-based biofilm matrix.

The human neck has relatively stable electrical characteristics as neck musculature is not strongly correlated with body type [19]. This is confirmed through dielectric probe measurement of four volunteers with BMI ranging between 20.5 and 44.9, Table 10.4. These relatively stable permittivity and conductivity values across human subjects have the benefit that unlike for other mounting points on the body, a single neck phantom can be utilised making a single tag design suitable for a wide variety of users.

10.1.1 Bio film sensor measurements

The Voyantic system demonstrated the sensing tag achieved read ranges of 65 and 80 cm at the 865 and 920 MHz bands, respectively, with good stability over triplicate tests. Figure 10.7 shows, that as the biofilm thickness increases, the reduction in read range at the two considered UHF bands corresponds to an increase in required

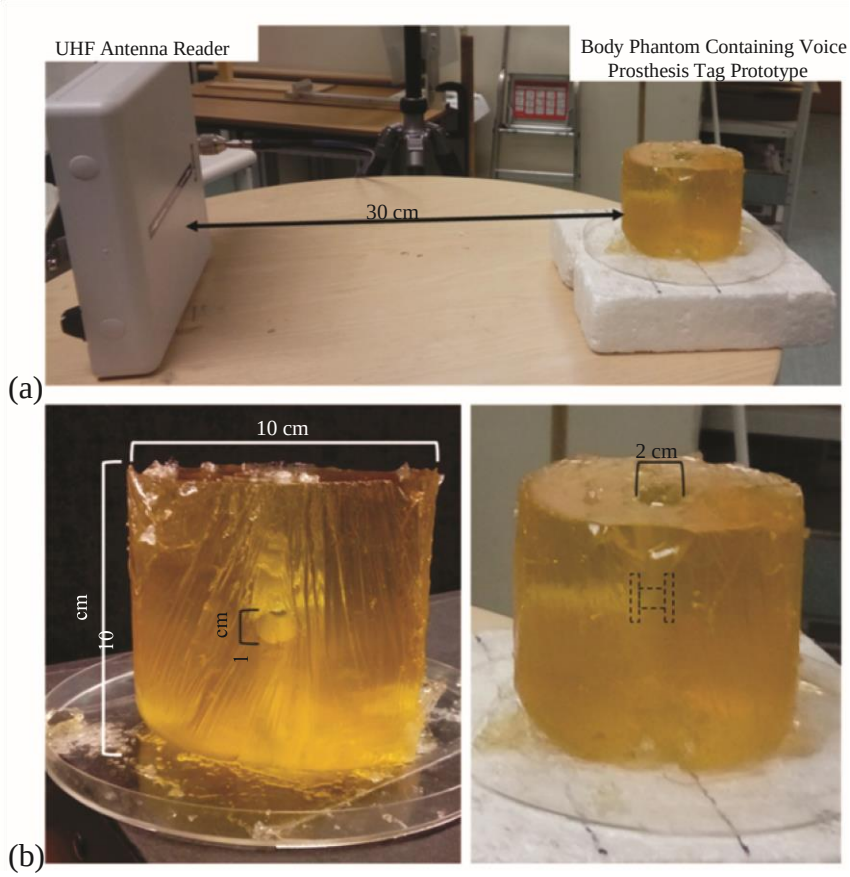

Figure 10.6 UHF RFID voice prosthesis prototype: (A) within a gelatin and salt neck phantom at 30 cm from the UHF antenna reader. (B) The 10 cm by 10 cm gelatin phantom was designed as a near human muscle replacement (58 permittivity and 1 S/m conductivity). Phantom contains a 2 cm vertical opening (modelling trachea) and 1 cm horizontal opening (modelling tracheostomy stoma). Prototype (dashed lines) placement is represented at the intersection between the two openings to module surgical placement of a standard voice prosthesis. Adapted with permission from [17]

Table 10.4 Electrical parameters of volunteer necks taken at 865 MHz

BMI	**Relative permittivity (293.75 K)**	**Conductivity (S/m)**
20.8	40.30 +/- 0.19	0.63 +/- 0.007
44.9	40.29 +/- 0.68	0.6 +/- 0.200
26.1	42.70 +/- 0.77	0.72 +/- 0.017
20.5	36.75 +/- 1.14	0.58 +/- 0.030
Average	40.1 +/- 2.31	0.64 +/- 0.058

*All readings represents averaged values taken in triplicate. ***Source*: data from [17].

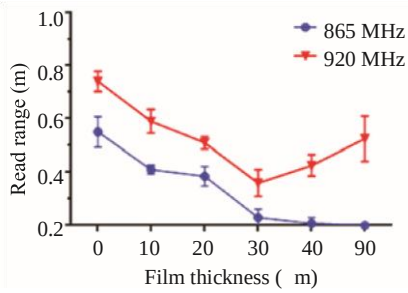

Figure 10.7 Emulated sensor response at EU and US RFID bands. Biofilm growth has been simulated by adding additional thicknesses of polyurethane to decouple the saliva layer (high dielectric constant) from the tag. It can be seen that as emulated biofilm growth increases (change in film thickness), the impedance mismatch (change in capacitance) shifts the frequency allowing for simple detection for any single frequency within the band of interest (source data from [17])

transponder activation power, and this is the sensor transfer response. The original tag tuning allows for unambiguous detection at both bands up to 30 mm biofilm thickness, and up to 40 mm for 865 MHz. Measuring films below this thickness is critical as they are associated with immature biofilms which might be treated with antifungal medication before they become mature and harden, leading to prosthetic valve failure. As this was a prototype, improved system robustness could be accomplished by utilising an RFID transponder capable of directly sensing changes in the antenna input reactance rather than relying on the required tag activation power which is affected by channel variations. However, this is one of the first UHF RFID designs to show detection of microbial growth while within human tissue.

In summary, a passive sensing tag has been shown to indicate the presence and thickness of a newly establishing fungal biofilm on a throat prosthesis and to be able to communicate wirelessly to an external RFID reader that does not need to be directly pressed against the skin. There is an advantage in the throat location of the implant as biological tissue parameters are much less of a function of body type than for other areas and this reduces the need to provide a comprehensive range of tuned tags. While this first prototype indicates biofilm thickness via link power parameters, future refinements could be made using capacitance sensing RFID transponders that digitally code the extent of detuning that they experience. The technology is proposed as a cost-effective means for a prosthesis user to self-manage the health of their device and reduce the need for surgical replacement.

10.2 Streaming Bio Data over Gen 2 RFID link

While the biofilm infection monitoring described in Section 10.1 is achieved through low sampling rates that suit the constraints of passive UHF RFID Gen2 protocol, there are epidermal sensors measuring parameters such as ECG (electrocardiography), EMG

(electromyography), EEG (electroencephalography), PPG (photoplethysmography) or accelerometery where there is a requirement to stream data. Skin patches worn for long periods require low profile flexible batteries. These cells have low capacities, and therefore power management becomes critical in low profile epidermal devices. A technique to achieve reliable streamed data transmission using RFID communication, Battery Assistive Passive (BAP) RFID is discussed in this section.

To harness the ultra-low power functionality of UHF RFID, while providing continuous data transmission with low latency, it is necessary to understand the available memory technologies and access procedures within the UHF RFID EPC Gen 2 protocol.

Typical RFID communications are based around static data being sent as an identifier. This means that items of merchandise, that have a static Electronic Product Code (EPC) [1] can be identified, logged, and located. Therefore, bursty low data rates are tolerated (in the region of 8–16 bytes of data), however the underlining fundamentals of the technology do allow for streaming dynamic data transfer at rates suitable for biological measurement, with examples including devices such as acceleration (60–200 Hz, 3 axis, 8–10 bit per axis) [20], Heart Rate data such as PPG [21], or ECG [22] in the range of 250 Hz at 8–10 bit resolution [23] (Figure 10.8). Typically, when looking at popular fitness devices within the

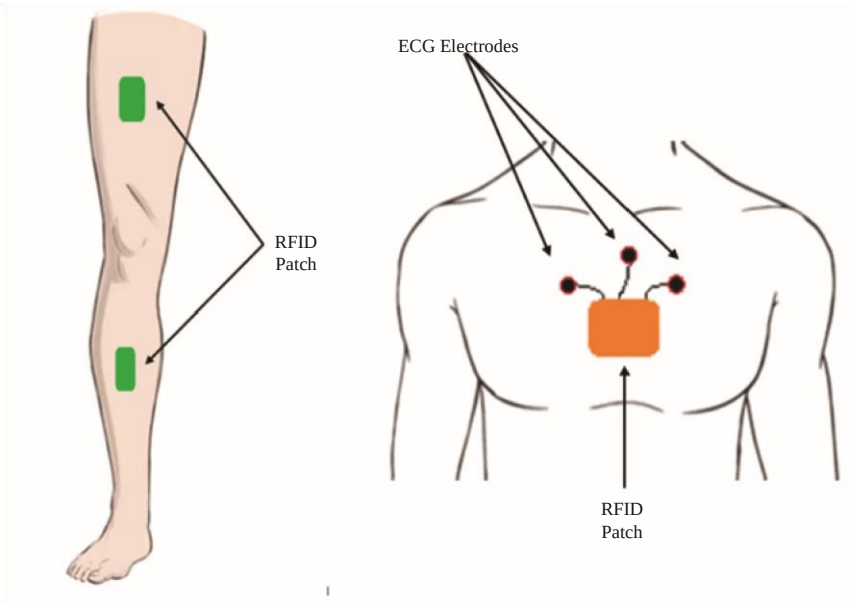

Figure 10.8 Mounting positions of two examples of streamed data RFID sensing modalities on the body, with dual attachment on the leg enabling three axis acceleration and singular chest attachment for EEG heart waveform

consumer market, transmission of this data off the body is achieved using low power versions of Bluetooth [24], however UHF RFID has the capability to send this data reliably and at a much lower power consumption [25].

Normal read requests access the tag transponder EEPROM (electrically erasable programmable read-only memory), which is a static memory type with a limited lifespan (100,000 read/write cycles) and moderate latency in performing functions (20–50 ms). For static data, or applications where data is not going to change frequently, this storage medium is more than sufficient, though when considering data that could be changing hundreds of times per second, its suitability diminishes. However, some RFID UHF chips offer a small region of memory located within the RAM registers. This is volatile memory and thus data is not retained when the device powers off, though compared to EEPROM, RAM has much lower read/write latency and the endurance is rated at 10,000,000,000 read/ write cycles. However, RAM has much lower memory per unit area than EEPROM, and devices which employ this memory type typically only have 16 Bytes available within the RAM.

When dealing with dynamic data, hardware additional to the RFID transponder is required including a microcontroller (MCU) to capture and process data from sensors and relay the information seamlessly to the RFID chip. One of the major roles of the MCU is to ensure that there are no data clashes when the remote reader is trying to communicate with the RFID Chip whilst the microcontroller is attempting to write new data. This would corrupt the data which then proves troublesome to validate, and results in either invalid information or a significant reduction in the overall operating speed of the device.

To overcome data clashing, a flag pin of the transponder chip can be used to regulate access to its volatile memory. The flag indicates when the tag transponder is communicating with the RFID reader and signals to the microcontroller that it should wait before attempting to access the transponder memory. This allows for a state machine to be defined that avoids clashes in the read/write cycles. When timed correctly, it facilitates low latency real-time data streaming from the sensing tags with no data clashes.

Figure 10.9 shows that there are essentially four prominent actors in the sampling of live data. To harness the full speed of a UHF RFID link, each stage has a prescribed set of instructions and purpose throughout the capture of raw data to its presentation at the remote computer.

To evaluate the system performance, an EM4325 RFID transponder from EM Microelectronics was connected to an MSP430FR5969 MCU from Texas Instruments. A high-performance computer was attached to the reader (Intel i9 7960x with 64 GB RAM) to reduce any latency that could be introduced into the system by slow USB polling. Figure 10.10 outlines the basic circuit implementation used to integrate all of the component parts of an example system to stream data. Figure 10.11 shows the physical hardware assembled with a monopole antenna and a large stitched ground plane. The hardware was moved in increments of 5 cm away from the reader to establish read speeds at varying ranges. A thingMagic M6E reader was used with a circular polarised antenna pointed at the monopole antenna.

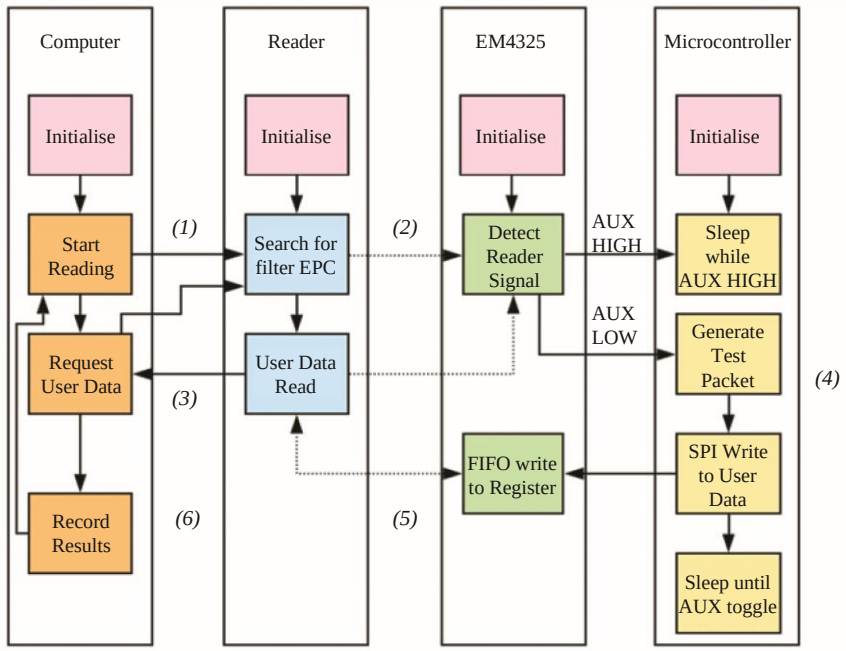

Figure 10.9 *System diagram of each stage for a single transaction of valid data, mimicking the transmission of body centric data from an RFID device. Sourced from [26]*

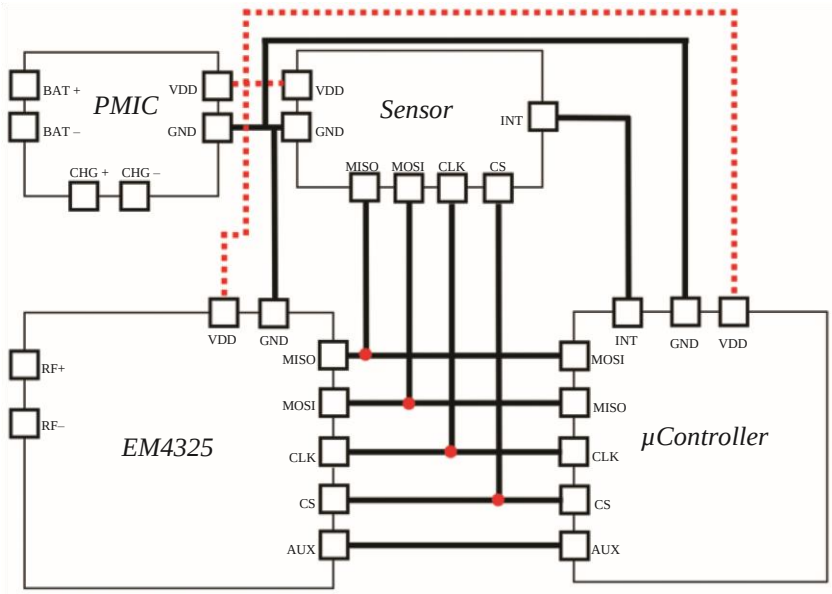

Figure 10.10 *System block diagram showing the interconnects between the power management integrated circuit (PMIC), sensor, EM4325 RFID chip and the microcontroller*

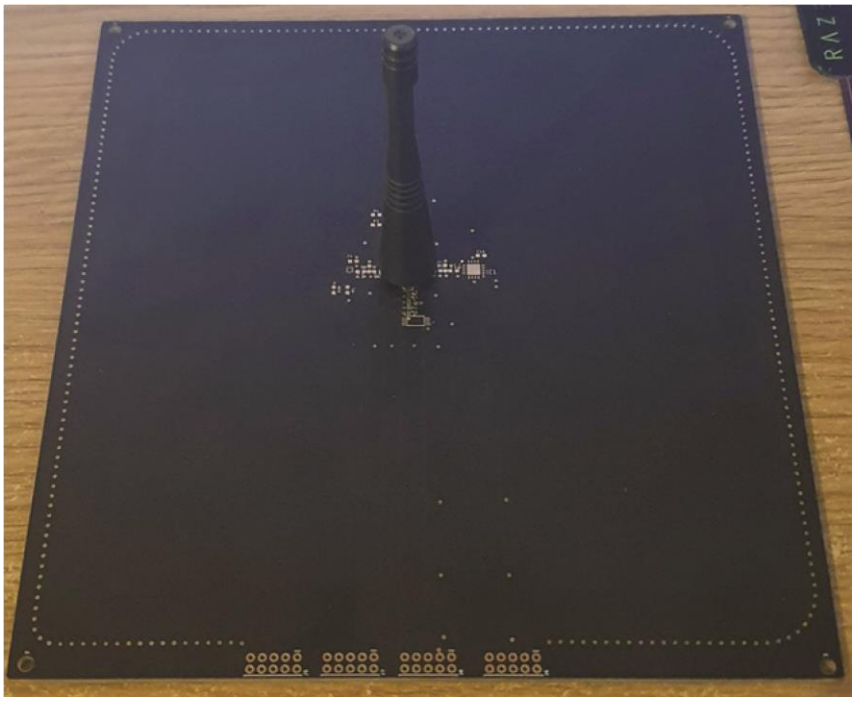

Figure 10.11 Dedicated RFID testing board with SMA connector for monopole antenna attachment and large ground plane. Sourced from [26]

The six main stages of the data management operation are discussed below:

1. Stage One: To begin, the computer would establish a serial connection with the reader via USB. Once the connection had been confirmed, settings for the reader would be sent detailing the use of battery assisted passive mode, fast search, *Q*-factor (0), BSK frequency (640 kHz), Hop table (2 hops) and the polling frequency (Maximum).
2. Stage Two: The reader would attempt to energise tags within the field, interrogating any tags with the specific EPC filter defined from the computer. This is to ensure the tag under test is the only one being engaged, as the performance can be degraded if other tags are within the field during the interrogation. The EM4325 then responds with its EPC and begins to toggle its internal AUX state.
3. Stage Three: Once the reader has established that the desired tag is within the field and able to return an EPC, a further request for tag data is sent. This request for data is pointed at the specific register section of the EM4325 for 16 bytes. The memory within this area is indexed in logical word addresses, resulting in a query of hex words 0 104 to 0 10B.
4. Stage Four: As the EM4325 transponder has detected the reader and toggled its AUX pin, the microcontroller can be brought out of a low power idle mode and

returned to normal operating speed. A test packet is then generated, which iterates upon every generation and is transmitted through SPI to the high speed 16 byte register of the EM4325. This transmission can only occur when the EM4325 AUX pin denotes that the reader is not actively communicating. This technique is used to stop both the microcontroller and the reader from accessing the same memory space simultaneously, causing a data deadlock. Once this transmission has occurred, the microcontroller can then resume its low power state to conserve battery power.

5. Stage Five: After the microcontroller has loaded the register, the reader will access the register, causing the AUX pin to flag that the register is unavailable.
6. Stage Six: Once the reader has captured the register data, it is then sent to the controlling computer which carries out a direct comparison with the previous frame of data to check whether the iteration of the frame contents matches. If it did not match, then it would be flagged and results in an error being presented to the tester, as well as being recorded. The data is logged into a .csv file for further offline processing.

Data sent via the communications line needs to be correctly packaged. The frame described in [26] was designed for data safety and only intended to send acceleration data at 60 Hz. It included frame number and CRC for added data integrity. However, the frame could be reconfigured and simplified to try and improve performance by only reading 7 bytes of data.

The frames were found to have an average latency of roughly 3 ms but with delay spikes of 6 ms and with occasional values above 10 ms. These spikes are observed for times when the reader is conforming to the EPC GEN2 standard. Read range, as shown in Figure 10.12 has good performance up until 2.5 m, whereby the transfer fails. It can be seen to recover at 2.55 m which is suspected to be the device moving out of a localised null, but the signal again fails and never recovers as distance increases. There is a minor penalty for using the full 16 bytes of the memory which can be seen in Figure 10.13 (A), but this is only around 10% of the update rate. It can also be seen in Figure 10.13 (B) that the effects of null regions

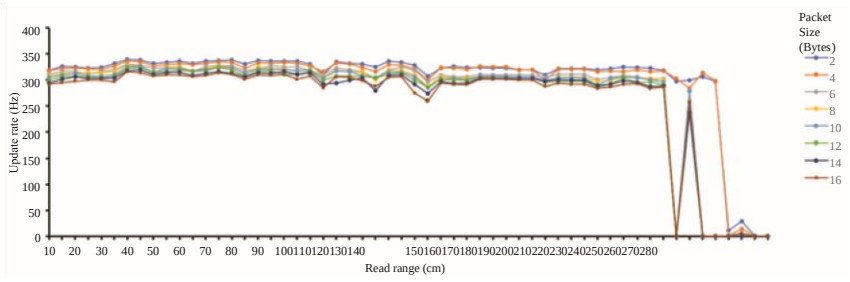

Figure 10.12 Update rate versus read range showing consistent speeds until 250 cm of EPC þ memory data in the eight packet sizes tested. Adapted from [26]

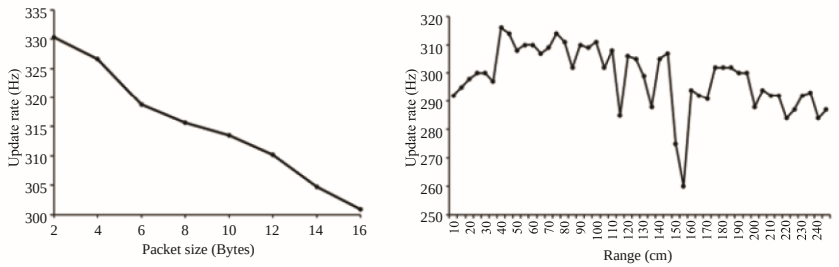

Figure 10.13 (A) Update rate versus packet size showing degradation in performance with increased packet size. (B) Update rate versus range with 16 byte packets showing effects of null regions on update rate. Adapted from [26]

can cause significant swings in data transfer rates (15%) and that the distance from the reader can cause further degradation.

Whilst the bulk of the results shown here are for in-air measurements, the indication of performance for body-worn applications which may degrade the Read Range cannot be ignored. A link speed of 16 bytes at 300þ times a second fulfils the EMG, ECG, PPG and accelerometry requirements with additional overhead to allow for error correction and recovery.

Furthermore, given the latency of around 3 ms per transmission, UHF data transfer offers significant improvement against Bluetooth low energy transfers with typical minimum values of around 5–6 ms with high likelihoods of large spikes in the 20 ms range [27].

10.3 Summary

This chapter has discussed two aspects of low power epidermally or conformally mounted UHF RFID sensing tag applications. First, colonising infections on voice prostheses can be detected using an entirely passive system by exploiting the thickening biofilm which decouples a saliva layer from the sensor tag antenna aperture fields. Obtaining passive backscattered UHF communications is challenging, though this voice prosthesis application benefits from both the relative stability in throat tissue electrical parameters in association with the low bulk density of the neck.

Second, for systems such as skin mounted accelerometry or ECG measuring tags, a microcontroller-based system can achieve streaming data at rates of 5.2 kB per second using RAM rather than EEPROM and avoiding clashes between the microcontroller and the RFID transponder chip. This technique has the potential for enabling low cost, compact and body conformal electronics in areas such as rapid diagnostics, where low overhead and instant response sensors are vital. Future investigations into this technique will aim to focus on optimised read/write cycles to improve read range and data throughput to the extent on which more advanced multicombination sensor suites might be achievable.

References

[1] Protocol U. EPC UHF Gen2 Air Interface Protocol | GS1 [Internet]. Gs1.org. 2022 [accessed 6 January 2022]. Available from: https://www.gs1.org/standards/rfid/uhf-air-interface-protocol

[2] Ziai M, Batchelor J. Temporary on-skin passive UHF RFID transfer tag. *IEEE Transactions on Antennas and Propagation.* 2011;59(10):3565–3571.

[3] Sanchez-Romaguera V, Wu¨nscher S, Turki B, *et al.* Inkjet printed paper based frequency selective surfaces and skin mounted RFID tags: the interrelation between silver nanoparticle ink, paper substrate and low temperature sintering technique. *Journal of Materials Chemistry C.* 2015; 3(9):2132–2140.

[4] Camera F, Miozzi C, Amato F, Occhiuzzi C, Marrocco G. Experimental assessment of wireless monitoring of axilla temperature by means of epidermal battery-less RFID sensors. *IEEE Sensors Letters*. 2020; 4(11):1–4.

[5] Kim D, Lu N, Ma R, *et al.* Epidermal electronics. *Science.* 2011; 333 (6044):838–843.

[6] Kellomaki T. On-body performance of a wearable single-layer RFID Tag. *IEEE Antennas and Wireless Propagation Letters.* 2012; 11:73–76.

[7] Ray T, Choi J, Bandodkar A, *et al.* Bio-integrated wearable systems: a comprehensive review. *Chemical Reviews.* 2019; 119(8):5461–5533.

[8] Amato F, Occhiuzzi C, Marrocco G. Epidermal backscattering antennas in the 5G framework: performance and perspectives. *IEEE Journal of Radio Frequency Identification.* 2020;4(3):176–185.

[9] Amato F, Amendola S, Marrocco G. Upper-bound performances of RFID epidermal sensor networks at 5G frequencies. In 2019 IEEE 16th International Conference on Wearable and Implantable Body Sensor Networks (BSN), 2019.

[10] Hughes J, Occhiuzzi C, Batchelor J, Marrocco G. Miniaturized grid array antenna for body-centric RFID communications in 5G S-band. In 2020 50th European Microwave Conference (EuMC), 2021.

[11] Colella R, Turmolo MR, Sabina S, et al . Design of UHF RFID sensor-tags for the biomechanical analysis of human body movements. *IEEE Sensors Journal.* 2021;13(21):14090–14098.

[12] Makarovaite V, Hillier A, Holder S, Gourlay C, Batchelor J. Passive wireless UHF RFID antenna label for sensing dielectric properties of aqueous and organic liquids. *IEEE Sensors Journal.* 2019;19(11):4299–4307.

[13] Oyeka D, Batchelor J, Ziai A. Effect of skin dielectric properties on the read range of epidermal ultra-high frequency radio-frequency identification tags. *Healthcare Technology Letters*. 2017;4(2):78–81.

[14] Makarovaite V, Gourlay C, Hillier A, Batchelor J, Holder S. Adjustable passive RFID skin mounted sticker. In: 2019 IEEE 16th International Conference on Wearable and Implantable Body Sensor Networks (BSN), 2019.

[15] Zuffanelli S, Aguila P, Zamora G, Paredes F, Martin F, Bonache J. An impedance matching method for optical disc-based UHF-RFID tags. In: 2014 IEEE International Conference on RFID (IEEE RFID), Apr 2014; pp. 15–22.

[16] Sidén Johan, Nilsson H-E.RFID antennas – possibilities and limitations. In: Radio Frequency Identification Fundamentals and Applications. London: INTECH Open Access Publisher; 2010; pp. 69–92.

[17] Makarovaite V, Hillier A, Holder S, Gourlay C, Batchelor J. Passive UHF RFID voice prosthesis mounted sensor for microbial growth detection. *IEEE Journal of Radio Frequency Identification.* 2020;4(4):384–390.

[18] Talpaert M, Balfour A, Stevens S, Baker M, Muhlschlegel F, Gourlay C. Candida biofilm formation on voice prostheses. *Journal of Medical Microbiology.* 2015;64(3):199–208.

[19] Kamibayashi L, Richmond F. Morphometry of human neck muscles. *Spine.* 1998;23(12):1314–1323.

[20] Taraldsen K, Chastin SF, Riphagen II, Vereijken B, Helbostad JL.Physical activity monitoring by use of accelerometer-based body-worn sensors in older adults: a systematic literature review of current knowledge and applications. *Maturitas.* 2012;71(1):13–19.

[21] Fortino G, Giampa` V. PPG-based methods for non-invasive and continuous blood pressure measurement: an overview and development issues in body sensor networks. In: 2010 IEEE International Workshop on Medical Measurements and Applications, New York, NY: IEEE; Apr 30 2010; pp. 10–13.

[22] Wong AC, McDonagh D, Omeni O, et al . Sensium: an ultra-low-power wireless body sensor network platform: design & application challenges. In: 2009 Annual International Conference of the IEEE Engineering in Medicine and Biology Society, New York, NY: IEEE; Sep 3 2009; pp. 6576–6579.

[23] Daskalov I, Christov I. Improvement of resolution in measurement of electrocardiogram RR intervals by interpolation. *Medical Engineering & Physics*. 1997;19(4):375–379.

[24] Kim H, Kim YS, Mahmood M, et al . Fully integrated, stretchable, wireless skin-conformal bioelectronics for continuous stress monitoring in daily life. *Advanced Science.* 2020; 7(15):2000810.

[25] Horne R, Batchelor J, Taylor P, Balaban E, Casson A. Ultra-low power on skin ECG using RFID communication. In: 2020 IEEE International Conference on Flexible and Printable Sensors and Systems (FLEPS), New York, NY: IEEE; Aug 16 2020; pp. 1–4.

[26] Horne R, Batchelor JC. A framework for a low power on body real-time sensor system using UHF RFID. *IEEE Journal of Radio Frequency Identification.* 2020;4(4):391–397.

[27] Rondon R, Gidlund M, Landernas K. Evaluating Bluetooth low energy suitability for time-critical industrial IoT applications. *International Journal of Wireless Information Networks.* 2017;24:278–290.